The EMBO Journal (2009) 28, 3439–3449 | © 2009 European Molecular Biology Organization | All Rights Reserved 0261-4189/09
www.embojournal.org

THE EMBO JOURNAL

Receptor quality control in the endoplasmic reticulum for plant innate immunity

Yusuke Saijo[1,*], Nico Tintor[1,3], Xunli Lu[1,3], Philipp Rauf[1,3], Karolina Pajerowska-Mukhtar[2,3], Heidrun Häweker[1], Xinnian Dong[2], Silke Robatzek[1] and Paul Schulze-Lefert[1,*]

[1]Department of Plant Microbe Interactions, Max Planck Institute für Züchtungforschung, Köln, Germany and [2]Department of Biology, Duke University, Durham NC, USA

Pattern recognition receptors in eukaryotes initiate defence responses on detection of microbe-associated molecular patterns shared by many microbe species. The Leu-rich repeat receptor-like kinases FLS2 and EFR recognize the bacterial epitopes flg22 and elf18, derived from flagellin and elongation factor-Tu, respectively. We describe Arabidopsis '*priority in sweet life*' (*psl*) mutants that show de-repressed anthocyanin accumulation in the presence of elf18. EFR accumulation and signalling, but not of FLS2, are impaired in *psl1*, *psl2*, and *stt3a* plants. *PSL1* and *PSL2*, respectively, encode calreticulin3 (CRT3) and UDP-glucose:glycoprotein glycosyltransferase that act in concert with STT3A-containing oligosaccharyltransferase complex in an N-glycosylation pathway in the endoplasmic reticulum. However, EFR-signalling function is impaired in weak *psl1* alleles despite its normal accumulation, thereby uncoupling EFR abundance control from quality control. Furthermore, salicylic acid-induced, but EFR-independent defence is weakened in *psl2* and *stt3a* plants, indicating the existence of another client protein than EFR for this immune response. Our findings suggest a critical and selective function of N-glycosylation for different layers of plant immunity, likely through quality control of membrane-localized regulators.

The EMBO Journal (2009) **28,** 3439–3449. doi:10.1038/emboj.2009.263; Published online 17 September 2009
Subject Categories: proteins; plant biology
Keywords: calreticulin; ER; immune receptor; LRR-RLK; MAMP

Introduction

A vital aspect of innate immunity in eukaryotes involves prompt detection of non-self structures derived from potential microbial intruders. Plants monitor encounters to potential threats derived from surrounding microbes by using two classes of immune receptors: pattern recognition receptors (PRRs) that directly recognize their cognate microbe-associated molecular patterns (MAMPs) and disease resistance (R) proteins that recognize the actions or structures of isolate/strain-specific pathogen effectors (Chisholm *et al*, 2006; Jones and Dangl, 2006; Boller and Felix, 2009). MAMP-triggered immunity (MTI) provides the first layer of inducible defence during plant–microbe interactions. Loss of single PRRs in Arabidopsis allows a significant increase in the invasion and propagation of pathogenic microbes in host tissues, providing evidence for a critical function of PRRs for host defence activity (Zipfel *et al*, 2004, 2006). Distinct PRRs trigger an almost identical set of physiological changes from seconds/minutes to hours/days on perception of their cognate MAMPs. Early responses such as changes in ion fluxes across the plasma membrane (PM), the generation of reactive oxygen species (ROS) and ethylene, and the activation of mitogen activated protein kinases (MAPKs) are followed by transcriptome reprogramming, metabolome changes including phytoalexin biosynthesis and callose deposition (Felix *et al*, 1999; Gomez-Gomez *et al*, 1999; Asai *et al*, 2002; Zipfel *et al*, 2006; Clay *et al*, 2009). These responses are thought to collectively enhance host immunity and thus represent hallmarks for MTI activation. However, it remains largely unknown whether and how those MTI-characteristic responses contribute to overall host defence activity and influence each other. Moreover, the molecular mechanisms by which a single PRR regulates multi-branched signalling pathways leading to such diverse outputs remain elusive.

Plants mount immune responses at the cost of other physiological processes such as growth and abiotic stress responses (Lozoya *et al*, 1991; Gomez-Gomez *et al*, 1999; McLusky *et al*, 1999; Asselbergh *et al*, 2008; Yasuda *et al*, 2008). Prolonged and/or de-regulated activation of immune receptors results in retardation of growth and abiotic stress responses, or occasionally cell death (Boller and Felix, 2009; Shirasu, 2009). Therefore, it is conceivable to presume that stringent quality control operates to prevent precocious activation of immune receptors in plants. In line with this notion, earlier studies have uncovered a critical function of the RAR1/SGT1/HSP90 chaperon complex for the abundance control of intracellular nucleotide-binding domain and LRR (NB-LRR)-containing R proteins (Shirasu, 2009). This chaperon complex has been described to serve to maintain the steady-state levels of intracellular R proteins in presumed pre-recognition complexes. However, whether or not this chaperon complex also modulates post-recognition signalling events of client R proteins is still unclear. On the other hand, very little is known about the mechanisms by which MAMP perception systems based on membrane-localized PRRs are established and maintained before and after their elicitation.

In eukaryotic cells, the majority of membrane-resident proteins undergo quality control during their folding and maturation in the endoplasmic reticulum (ER) termed ERQC

*Corresponding authors. Y Saijo or P Schulze-Lefert, Department of Plant Microbe Interactions, Max Planck Institute für Züchtungforschung, 50829 Köln, Germany. Tel.: +49 221 5062 337; Fax: +49 221 5062 353; E-mail: saijo@mpiz-koeln.mpg.de
or Tel.: +49 221 5062 350; Fax: +49 221 5062 353; E-mail: schlef@mpiz-koeln.mpg.de
[3]These authors contributed equally to this work

Received: 21 June 2009; accepted: 6 August 2009; published online: 17 September 2009

(Hebert and Molinari, 2007; Anelli and Sitia, 2008; Pattison and Amtmann, 2009). ERQC ensures the delivery of only properly folded proteins to their functional sites and elimination of potentially detrimental, misfolded proteins through the ER-associated degradation (ERAD) pathway. At least, several different mechanisms have been described in parallel to execute ERQC in animal cells (Hebert and Molinari, 2007; Anelli and Sitia, 2008). One of the well-studied ERQC pathways is characterized by Asn (N)-linked glycosylation of the nascent client proteins. N-glycosylation is catalysed by the oligosaccharyltransferase (OST) complex, of which one subunit is defined by STT3, that transfers a preassembled glycan chain ($Glc_3Man_9GlcNAc_2$) to N-residues in the sequon N-X-Ser/Thr (X is except Pro) of acceptor proteins. Subsequent trimming of terminal glucose residues produces mono-glucosylated glycans ($Glc_1Man_9GlcNAc_2$) on the client proteins, thereby facilitating their recognition and folding by the ER-resident lectin-like chaperons calnexin (CNX) and calreticulin (CRT). Removal of the outermost glucose residues allows $Man_9GlcNAc_2$-conjugated client proteins to be released from the chaperons. Properly folded proteins are transferred to their functional sites through the endo-membrane (EM) system, whereas incompletely folded proteins with hydrophobic regions exposed are recognized by the ER lumen enzyme UDP-glucose:glycoprotein glucosyltransferase (UGGT). UGGT attaches a glucose residue to N-linked $Man_9GlcNAc_2$ glycans of client proteins, and then produces mono-glucosylated glycans that again facilitate the client proteins to enter reiterated cycles of CNX/CRT-assisted folding, designated the CNX/CRT cycle. It also defines a checkpoint at which unfolded proteins are retained in the ER for additional folding attempts or targeted for degradation in the cytoplasm through ERAD.

In Arabidopsis, several *uggt* mutant alleles have been described as allele-specific suppressor of a chemically induced mutant version of the brassinosteroid (BR) receptor (*bri1-9*) (Jin *et al*, 2007). This defective receptor variant undergoes UGGT-dependent retention in the ER because of improper folding. This finding suggests a potential function of the CNX/CRT/UGGT cycle in the ERQC of LRR-RLKs, of which some members act as PRRs, in plants. However, of note, loss of UGGT shows no discernable defects in BR-mediated processes in the wild-type (WT) *BRI1* background, indicating that this LRR-RLK is not a physiological client of UGGT. To our knowledge, a physiological client of the plant CNX/CRT/UGGT cycle has not been genetically defined to date.

Elucidation of regulatory mechanisms underlying MTI is fundamentally important for understanding the nature of plant innate immunity, as MTI provides an evolutionary basis of and functional links to different layers of plant immunity such as R protein-triggered immune responses and SA-induced defence (Chisholm *et al*, 2006; Mishina and Zeier, 2007; Shen *et al*, 2007; Tsuda *et al*, 2008). Although an increasing list of PRRs and their co-receptor have been identified (Chinchilla *et al*, 2007; Heese *et al*, 2007), the lack of systematic genetic studies has hampered further identification of elements required for MTI. Here, we have taken a genetic approach to identify and isolate Arabidopsis mutants that are insensitive to MAMPs, focusing on the two best-studied MAMP/PRR pairs in plants flg22/FLS2 and elf18/EFR. Our genetic screens have revealed a selective key function of CRT3, UGGT, and STT3A that act in concert in an ER-resident N-glycosylation pathway for the biogenesis and function of EFR, but not FLS2. Furthermore, we have found that UGGT and STT3A are required for an EFR/FLS2–independent, but SA-dependent defence, indicating potential engagement of this ERQC pathway and its client membrane proteins in the control of different layers of plant immunity.

Results and discussion

A genetic screen based on MAMP-sucrose signalling crosstalk identifies elf18-insensitive psl mutants

In an attempt to dissect PRR-mediated MTI, we have performed genetic screens for MAMP-insensitive plants. A crosstalk between MAMP signalling and abiotic stress-induced flavonoid accumulation has been described in a wide range of plant–microbe interactions (Lozoya *et al*, 1991; Lo and Nicholson, 1998; McLusky *et al*, 1999). Light-induced anthocyanin accumulation is enhanced by high concentrations of sucrose (Tsukaya *et al*, 1991). However, the sucrose effect is abolished in young Arabidopsis seedlings in the presence of the bacterial MAMPs flg22 and elf18 (Figure 1A). On the basis of these findings, we have screened $>60\,000$ ethylmethanesulfonate-mutagenized M_2 seedlings for plants defective in this crosstalk. We identified >50 '*priority in sweet life*' *(psl)* mutants that show de-repression of anthocyanin accumulation in the presence of elf18, but retain flg22-dependent repression (Figure 1B and C; Supplementary Figure S1A). The *psl* plants do not constitutively produce anthocyanins at high levels (Figure 1C). They represent more than three complementation groups, including novel *efr* alleles as well as non-receptor *psl1* and *psl2* mutants (Table I). The results indicate that separate genetic requirements exist between FLS2 and EFR functions. This was unexpected, as these PRRs are highly related in overall structure and have been claimed to activate shared signalling pathways (Zipfel *et al*, 2006).

We next tested whether *psl1* and *psl2* plants are altered in characteristic MAMP-induced events. Strong alleles of *psl1* and *psl2* plants fail to induce detectable ROS generation in leaves in response to elf18 (Figure 1D; Supplementary Figure S1B). Elf18-induced MAPK activation is diminished in young seedlings of both mutants (Figure 1E). PMR4/GSL5-mediated callose deposition (Kim *et al*, 2005), a late elf18-induced response, is also abolished in these plants (Figure 1F). However, both *psl1* and *psl2* plants retain WT-like responsiveness to flg22 in all these assays (Figure 1D–F). This suggests that the mutants are specifically impaired in EFR-mediated signalling upstream of general machineries that execute those responses.

To ensure the functional significance of these observations, we have tested the immune activity of the *psl* plants. Earlier studies have rather suspected a function of EFR in host immunity against the virulent bacterial phytopathogen *Pseudomonas syringae* pv. *tomato* (*Pst*), as potential epitopes derived from EF-Tu of *Pst* are less potent for EFR elicitation than elf18 derived from that of *Escherichia coli* when exogenously provided (Kunze *et al*, 2004; Zipfel *et al*, 2006). However, it remains unclear whether and how these epitopes are exposed to PRRs during the pathogen infection. Remarkably, *efr* plants allow high propagation of the bacteria under our assay conditions, in which we use high dosage (10^9 cfu/ml) of the bacteria for spray inoculation and keep

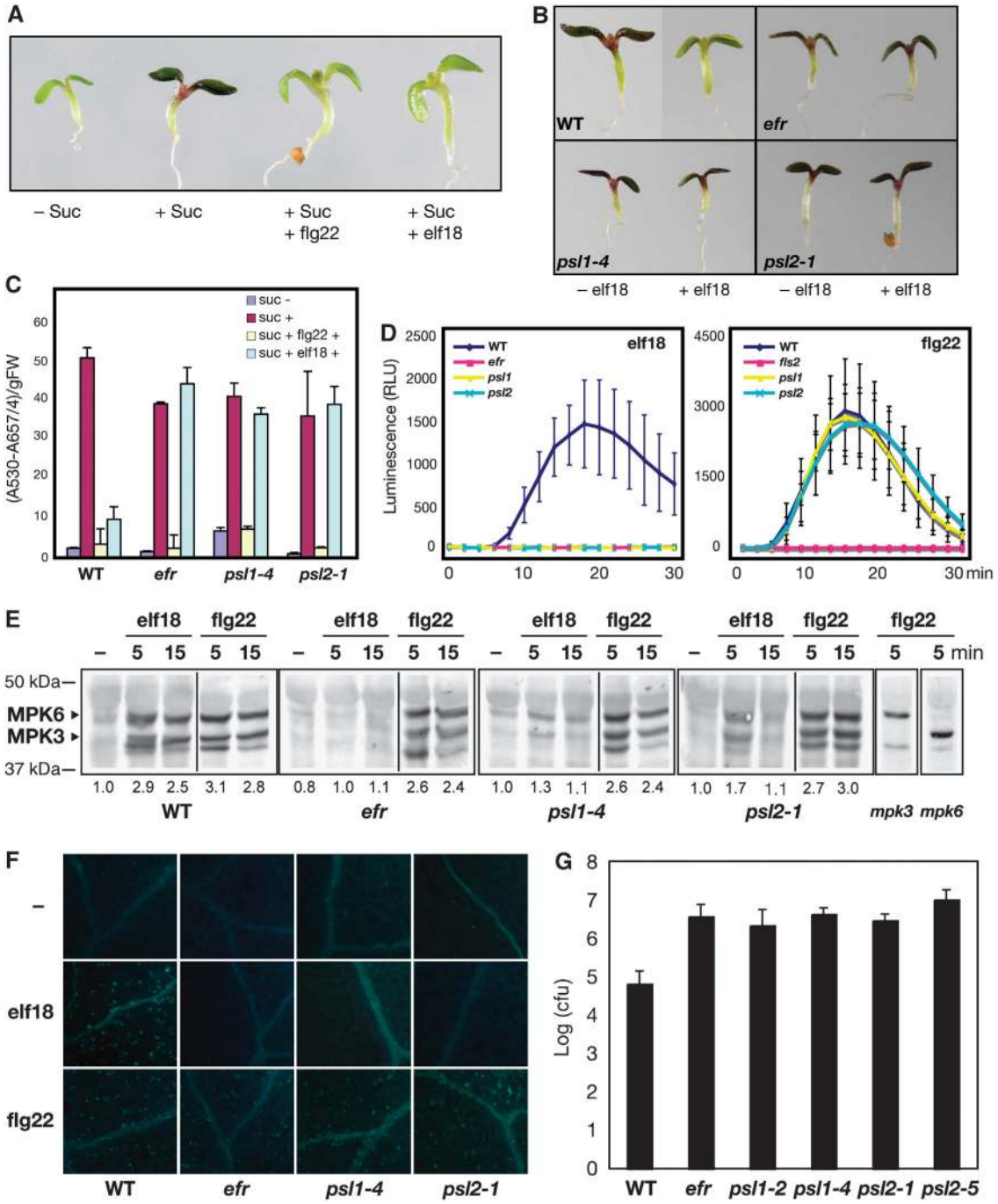

Figure 1 Arabidopsis non-receptor mutants specifically impaired in EFR-triggered immune responses. (**A**) Wild-type (WT; Col-0) seedlings grown in the absence of sucrose (− Suc) or presence of 100 mM sucrose (+ Suc) without or with 1 μM flg22 (+ flg22) or elf18 (+ elf18). (**B**) Effects of 1 μM elf18 on sucrose-induced anthocyanin accumulation in WT, *efr-1* (*efr*), *psl1-4*, and *psl2-1* mutants. (**C**) Anthocyanin content in 6-day-old seedlings grown as described in (A). (**D**) ROS generation triggered in leaf discs of the WT, *efr*, *fls2*, *psl1-4* (*psl1*), and *psl2-1* (*psl2*) plants at 100 nM elf18 or flg22. (**E**) MAPK activation in WT, *efr*, *psl1-4*, *psl2-1*, *mpk3*, and *mpk6* seedlings on application of water for 5 min (−), 1 μM elf18 or flg22 for the indicated times. All samples on a panel are derived from the same gel. Positions of molecular weight markers are shown on the left. Numbers under immunoblots indicate relative MPK6 band intensities that were normalized with the WT mock control (=1.0). (**F**) Callose deposits stained with aniline blue in the cotyledons of WT, *efr*, *psl1-4* and *psl2-1* seedlings treated with water (−), 1 μM elf18 or flg22 for 20 h. (**G**) Growth of *Pst* DC3000 in 4-week-old plant leaves 3 days after spray infection with bacteria at 1×10^9 cfu/ml.

the plants under high humidity throughout the infection procedure (Figure 1G; see Materials and methods). Consistent with the observed deficiency in the elf18-induced events examined, both *psl1* and *psl2* plants exhibit robust super-susceptibility on challenge with *Pst*, at comparable levels to that of *efr* plants (Figure 1G). This supports functional requirements of *PSL1* and *PSL2* for MTI. Taken together, our genetic evidence identifies these two genes as non-receptor components specifically required for EFR-mediated immunity.

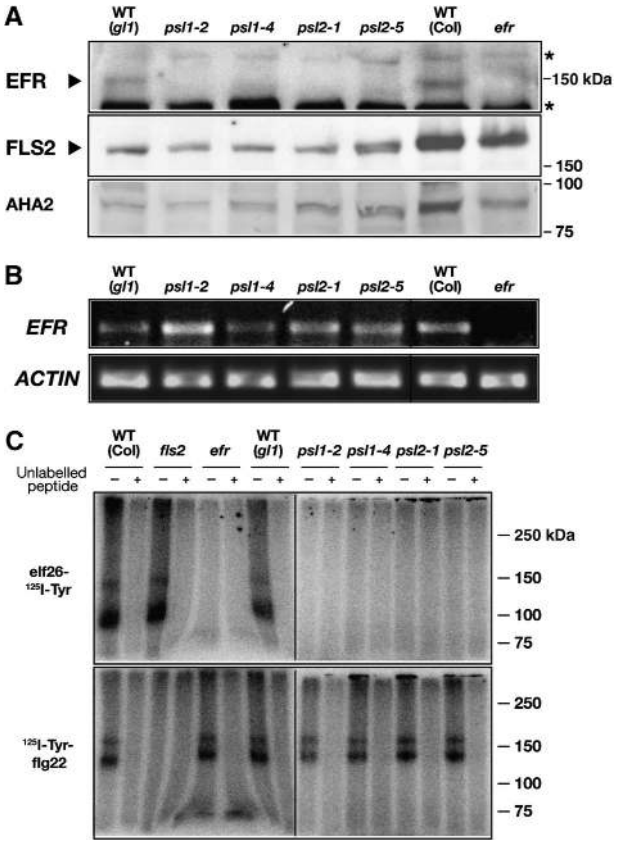

Figure 2 PSL1 and PSL2 are required for stable accumulation of functional EFR. (**A**) Immunoblot analysis of microsomal membrane fraction derived from 4-week-old non-elicited plants with anti-EFR, FLS2, and H^+-ATPase2 (AHA2) antibodies. Asterisks indicate the positions of cross-reacting bands with the EFR antibodies. Positions of molecular weight markers are shown on the right. (**B**) Semi-quantitative RT–PCR analysis for *EFR* expression of the samples used for (A). (**C**) *In vitro* chemical cross-linking of extracts from 2-week-old seedlings with the radio-labelled elf26 or flg22 probes in the absence (−) or presence (+) of 10 μM unlabelled competitor peptides elf18 or flg22, respectively. Elf26- and flg22-probed samples were, respectively, analysed together side by side.

Both PSL1 and PSL2 are required for stable accumulation of functional EFR but not FLS2

The vast defects from early to late elf18-triggered responses in the *psl* mutants (Figure 1D–F) prompted us to examine possible alterations at the level of the receptor. We have developed the procedures using specific anti-EFR antibodies to monitor the endogenous EFR protein in immunoblot analysis. We detect a signal for EFR in the microsomal membrane fraction, but not soluble fraction (not shown), derived from leaves of non-elicited WT plants (Figure 2A). Its apparent size is approximately 145 kDa and larger than its predicted size of 113 kDa. The steady-state levels of EFR are greatly reduced in strong alleles of both *psl1* and *psl2* plants (Figure 2A) without a significant decrease in the *EFR* transcript levels (Figure 2B), indicating that the mutants are impaired at a post-transcriptional step in receptor biogenesis. However, the mutants show no clear difference in the abundance of FLS2 (Figure 2A), again pointing to the specific requirements of PSL1 and PSL2 for EFR function. The same conclusion has been obtained with elf18-stimulated plants (Supplementary Figure S2).

We then determined the ligand-binding activity in those mutants by *in vitro* incubation of plant protein extracts with radio-labelled elf26 (equivalent to elf18) or flg22 as ligands. As earlier described (Chinchilla *et al*, 2006; Zipfel *et al*, 2006), we detected double bands at approximately 150 and 100 kDa for elf26, and 175 and 140 kDa for flg22, respectively, in our cross-linking experiments using protein extracts from whole plants (but not from cell culture). In either case, it is unclear whether both forms exist *in vivo*. Nonetheless, both bands are specific because they are absent in respective *efr* and *fls2* mutant samples and are competed on addition of unlabelled elf18 and flg22 peptides. Consistent with the observed decrease in EFR abundance, EFR-dependent elf26 binding, but not FLS2-dependent flg22 binding, is greatly diminished in the *psl* mutants (Figure 2C). Together, we conclude that PSL1 and PSL2 are required for stable accumulation of functional EFR.

Identification of PSL1 and PSL2 reveals an essential function of CRT3 and UGGT for stable accumulation of EFR

We identified both *PSL* genes by positional cloning and subsequent recovery of multiple alleles (Figure 3A and B). *PSL1* encodes one of the three CRTs in Arabidopsis (Persson *et al*, 2003), designated CRT3 (At1g08450) (Figure 3A). Vertebrate CRT recognizes client proteins conjugated with N-linked mono-glucosylated ($Glc_1Man_9GlcNAc_2$) glycans and facilitates their proper folding (Hebert and Molinari, 2007; Anelli and Sitia, 2008). Despite a similar degree of elf18 insensitivity (Supplementary Figure S1 and Table I), plants containing the severe *psl1-2* and *psl1-4* alleles accumulate CRT3 at undetectable and normal levels, respectively (Figure 3C). *PSL2* encodes the ER lumen enzyme UGGT (At1g71220), the only UGGT homologue annotated in Arabidopsis (Figure 3B). In animal cells, it has been well documented that CRT and UGGT work in concert as a part of the ERQC mechanisms that ensure the proper folding of N-glycosylated proteins. These *psl1* and *psl2* alleles show no obvious effects on plant development and growth under the laboratory conditions (not shown), consistent with earlier described *uggt* alleles in Arabidopsis (Jin *et al*, 2007). This is in sharp contrast to the *uggt* and *crt* knockout mice that show embryonic lethality, which hampers further in-depth studies in a whole organism context (Anelli and Sitia, 2008).

To test the hypothesis that EFR biogenesis occurs through the CRT3/UGGT cycle, we first examined the distribution of endogenous EFR and CRT3 in different membrane compartments. Two-phase partitioning experiments with microsomal protein extracts from non-elicited plants detected a portion of EFR in the upper PM-enriched phase as well as the PM marker H^+ATPase2. EFR was also present with the ER marker CRT1 in the lower EM-enriched phase (Figure 3D). As predicted, CRT3 was exclusively detectable in the EM-enriched fraction. At present it is unknown which fraction represents a functional site of EFR. In this regard, we notice an apparent high recovery of EFR in the EM versus PM fractions as compared with the PM marker used. A significant portion of the immune receptor might thus be constitutively pooled in the EMs.

Severe defects in EFR accumulation in the presence of dysfunctional CRT3/UGGT cycle suggest an operation of stringent ERQC that directs improperly folded EFR to degra-

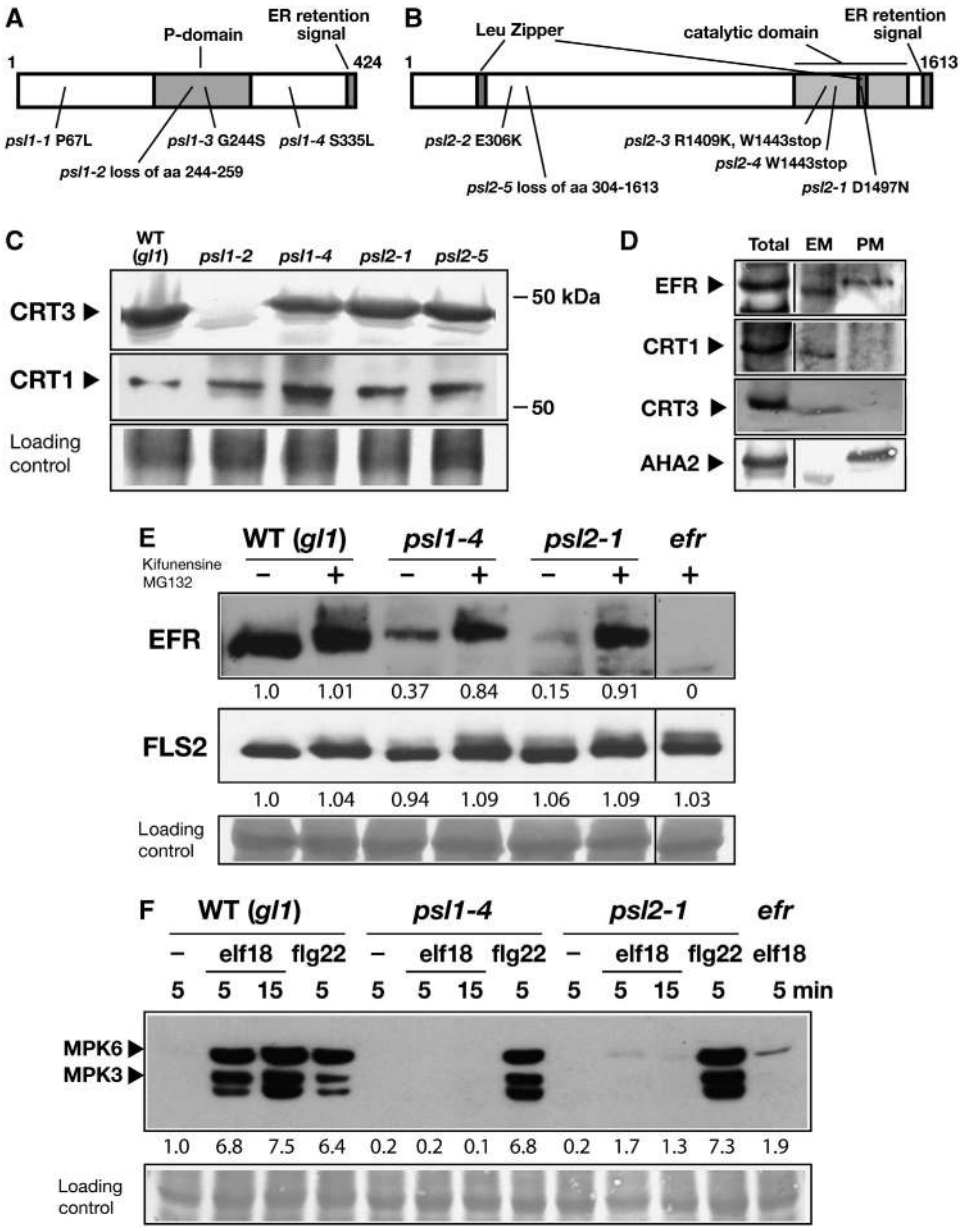

Figure 3 The CRT3/UGGT cycle-mediated quality control of EFR. (**A**, **B**) Schematic description of the structure of CRT3 (A) and UGGT (B). CRT3 (424 amino-acid residues; aa) is characterized by the P-domain and C-terminal ER retention signal. UGGT is characterized by two Leu Zipper motifs, C-terminal catalytic domain and the ER retention signal. Positions of changes in aa in the isolated alleles for *psl1* (A) and *psl2* (B) mutants are shown at the bottom. (**C**) Immunoblot analysis of membrane fractions from non-elicited leaves of 4-week-old plants with the indicated antibodies on the left. (**D**) Two-phase partitioning analysis of membrane fractions from non-elicited leaves of 4-week-old WT plants. Total, EM, and PM, respectively, represent total microsomal membrane, EM-enriched, and PM-enriched fractions. Immunoblots probed with anti-EFR, CRT1, CRT3, and AHA2 antibodies are derived from one gel, respectively. This loading represents overloading of the PM fraction by approximately eight-fold on a per-tissue amount basis. Apparent size difference between the EM and PM fractions is typical with this analysis, reflecting their different buffer composition. (**E**) Immunoblot analysis of total protein lysates from 2-week-old seedlings treated with kifunensine at 40 μM and MG132 20 μM for 24 h. (**F**) Plants prepared as described in (E) were elicited with 1 μM elf18 or flg22 for the indicated times and then subjected to immunoblot analysis with anti-active MAPK antibodies. Numbers under the blots in (E) and (F) indicate relative band intensities of EFR, FLS2, or MPK6 that were normalized with the WT mock control (= 1.0).

dation. We indeed verified that EFR accumulates at almost WT-like levels in *psl1* and *psl2* plants when pre-treated with kifunensine and MG132 (Figure 3E), inhibitors of ER and Golgi α-1,2-mannosidases and the proteasome, respectively, that collectively prevent ERAD in Arabidopsis (Hong *et al*, 2008). In the liquid culture containing these inhibitors, WT plants show robust MAPK activation in response to elf18 or flg22 (Figure 3F). However, despite the restoration of EFR accumulation, both *psl* plants are unable to induce MAPK activation on elf18 elicitation (Figure 3F). Thus, this stabilized EFR seems to be defective in signalling. It is also possible that signalling-competent EFR is stabilized, but retained in the ER when ERAD is blocked in these *psl* plants. Nevertheless, these data strongly indicate that EFR is actively eliminated through ERAD in the absence of the proper CRT3/UGGT cycle.

EFR function is impaired in the presence of weak psl1 (crt3) alleles without a clear decrease in its steady-state levels

Remarkably, weakly defective *psl1* alleles are partially and differentially impaired in elf18-induced responses without significant alterations in the steady-state levels of EFR in the absence (not shown) or presence of elf18 stimulation (Figure 4A). In *psl1-1* plants, ROS generation is retained at intermediate levels, whereas MAPK activation as well as callose deposition is much reduced (Figure 4B–D). It seems that ROS generation occurs without robust MAPK activation, although earlier studies have claimed that MAPKs act upstream of ROS generation (Zhang *et al*, 2007). There might be possible differences between EFR- and FLS2-initiated signalling that reconcile the discrepancy between these two data sets. On the other hand, despite nearly WT-like ROS and MAPK induction, in *psl1-3* plants, callose deposition is significantly reduced albeit detectable (Figure 4B–D). This sug-

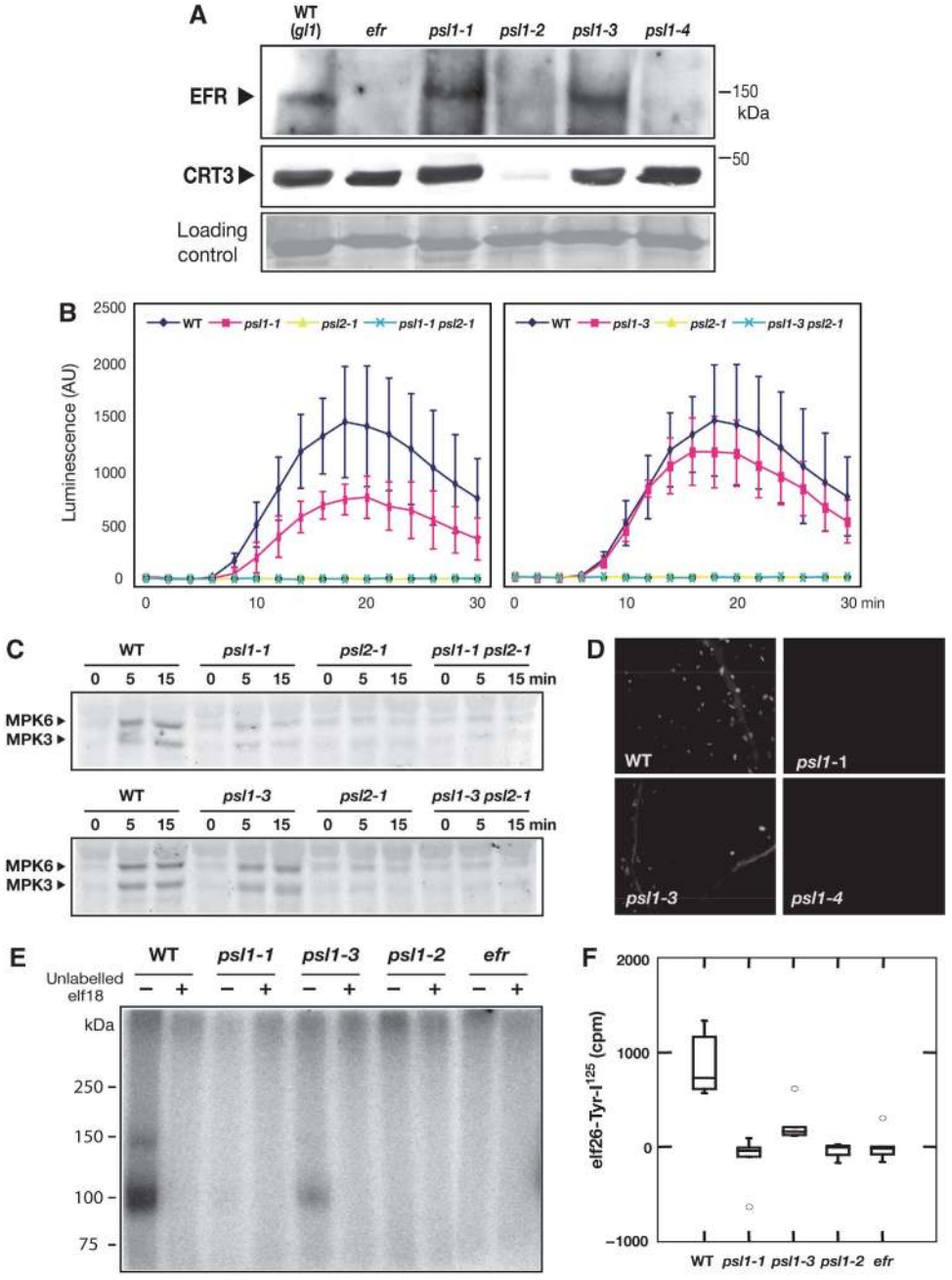

Figure 4 Characterization of *psl1* weak alleles and *psl1 psl2* double-mutant plants. (**A**) Immunoblot analysis of microsomal membrane fraction from 4-week-old plant leaves with elf18 elicitation at 0.5 μM for 24 h. Antibodies used and the positions of molecular weight markers are shown on the left and right, respectively. (**B**) ROS generation triggered in leaf discs derived from 4-week-old plant leaves on 100 nM elf18. (**C**) MAPK activation in 2-week-old seedlings triggered by elf18 at 1 μM for the indicated times. Plant protein lysates were subjected to immunoblot analysis with anti-active MAPK antibodies. (**D**) Callose deposits stained with aniline blue in cotyledons of WT and *psl1* seedlings treated with 1 μM elf18 for 20 h. (**E**) *In vitro* chemical cross-linking of extracts from 2-week-old non-elicited seedlings with the radio-labelled elf26 ligand in the absence (−) or presence (+) of 10 μM unlabelled competitor peptide. (**F**) Specific elf26 binding activity of plant extracts. The squares denote the median for two biological independent experiments with three technical replicates. The circles denote single outliers excluded from the calculation.

gests that even co-activation of ROS production and MAPK are insufficient to induce callose deposition at normal levels.

Another inference from our data is that the abundance control and quality control of EFR can be uncoupled, and that only the latter is influenced in the presence of weak *psl1* alleles. The LRR domain of EFR is likely exposed to the extracellular surface at the PM and serves as the ligand-binding site(s). If the topology of the immune receptor is as such, then it should be the LRR domain that undergoes CRT3/UGGT-mediated ERQC. We thus examined the ligand-binding activity of EFR in the presence of these *psl1* alleles. Strikingly, specific elf26 binding is nearly at the background level in *psl1-1* and drastically reduced in *psl1-3* mutants under our assay conditions (Figure 4E and F). Milder effects on elf18-induced responses by *psl1-3* as compared with *psl1-1* mutations may reflect the residual-ligand-binding activity detected in the former (Figure 4B–D). However, ligand binding must occur in *psl1-1* mutants as well below the detection limit of our assay as ROS generation is induced by elf18 (Figure 4B). Taken together, it seems likely that partial loss of CRT3 functions results in improper folding of the EFR LRR domain, thereby reducing ligand binding of the receptor.

PSL1/CRT3 and PSL2/UGGT act in concert for EFR function

We next obtained genetic evidence for functional interactions between CRT3 and UGGT by using a series of *psl1 psl2* double mutants. The residual activity in elf18-induced ROS generation and MAPK activation in weak *psl1-1* and *psl1-3* alleles is totally abolished in the *psl2-1* mutant background (Figure 4B and C). There is no additive increase of de-repressed anthocyanin levels by a combination of two strong alleles in *psl1-4 psl2-1* double-mutant plants as compared with the parent single mutants (Supplementary Figure S3). These results support our model in which CRT3 and UGGT work in concert to establish EFR function.

EFR is more vulnerable than FLS2 to perturbations of N-glycosylation

We addressed a possible basis for the observed difference between EFR and FLS2 in their dependence on specific components of ERQC. A number of N-glycosylation sites (N-X-S/T in which X is other than P) are predicted on the LRR domain of both PRRs. Peptide N-glycosidase treatment of plant protein lysates detected a decrease of apparent EFR size in immunoblot analysis (Figure 5A), showing that N-glycosylation indeed occurs on both EFR and FLS2 *in vivo*. We then suspected that EFR and FLS2 might differ in sensitivity to perturbations of N-glycosylation. In Arabidopsis, loss of a catalytic subunit of OST, STT3A, results in under-N-glycosylation of the mutant proteome and salt/osmotic stress sensitivity in the mutant plants (Koiwa *et al*, 2003). Similar to *psl1* and *psl2* plants, *stt3a-2* plants show de-repressed anthocyanin accumulation in the presence of elf18, but not of flg22 (Figure 5B). Immunoblot analysis revealed a dramatic decrease in the steady-state levels of EFR in these mutants (Figure 5C). On the other hand, the abundance of FLS2 and CRT3 is not significantly lower in *stt3a* plants as compared with the WT plants (Figure 5C). As EFR mRNA levels are not decreased in *stt3a* plants (Figure 5D), our data indicate that EFR accumulation is highly vulnerable to alterations in STT3A-dependent N-glycosylation among the membrane proteins tested. Consistent with this, EFR- but not FLS2-initiated ROS generation and MAPK activation are impaired in *stt3a* plants (Figure 5E and F). As predicted from these defects in EFR-mediated signalling, *stt3a* plants were found to be hypersusceptible to *Pst* (Supplementary Figure S4).

UGGT and STT3A contribute to EFR/FLS2-independent but SA-dependent immunity

Given the lack of obvious pleiotropic defects in *psl* mutants under normal growth conditions, we speculated that PSL-mediated ERQC becomes rate limiting under stress conditions. It has been reported that the induction of protein secretory machineries including the ER chaperone BiP2 promotes SA-mediated systemic acquired resistance (SAR) (Wang *et al*, 2005). It is known that exogenous application of SA enhances plant defence through a process shared by SAR (Loake and Grant, 2007). We thus tested possible alterations in the *psl* mutants of SA-induced resistance against the virulent strain *P. syringae* pv. *maculicola* ES4326. Although SA pre-treatment enhances immune responses against subsequent bacterial infection in *fls2*, *efr* and *psl1* plants as well as in the WT control, *psl2* plants remain highly susceptible (Figure 6A). In addition, *stt3a-2* plants also show a significant decrease of the SA effect on immunity (Figure 6B). Under our assay conditions, we fail to see clear SA-induced resistance in the WT C24 accession as well as in *stt3a-1* plants (not shown). Nevertheless, our data suggest that UGGT and STT3A, but not CRT3 and the PRRs, are required for this SA-induced immune response. The observed dispensability for CRT3 may be explained by possible redundancy among the ER lectin-like chaperones (three copies of CRTs and two copies of CNXs in Arabidopsis) that can work in concert with UGGT in the folding/maturation of N-glycosylated client proteins (Persson *et al*, 2003; Pattison and Amtmann, 2009). Our data predict the existence of another client protein than EFR for UGGT/STT3A-mediated ERQC that acts as a membrane localized or secreted regulator for SA-induced immune responses.

Concluding remarks

Our results reveal a key function of the CRT/UGGT cycle-mediated ERQC and STT3A-dependent N-glycosylation for two fundamental branches of plant immunity: MTI and SA-induced immunity. In the accompanying paper, Nekrasov *et al* (2009) also show a function of two other ERQC components and STT3A for MTI. Immune receptors are subject to ongoing selection during host–microbe co-evolution in which it is desirable to test cryptic structural variants. However, it is also essential to avoid their precocious activation leading to cell death or growth arrest. Elaborate quality control of immune sensors would be required to establish such evolutionary capacitance. We have shown in this study that active elimination of mal-folded, non-functional receptor protein occurs for EFR (Figure 3E and F).

Our data show that the biogenesis of EFR, but not FLS2 strictly relies on a subset of ERQC components despite a high similarity in their overall structure. This seems to render the former PRR more sensitive than the latter to perturbations of cellular N-glycosylation activity. It is known that flg22 responsiveness and FLS2 orthologues are present in a wide

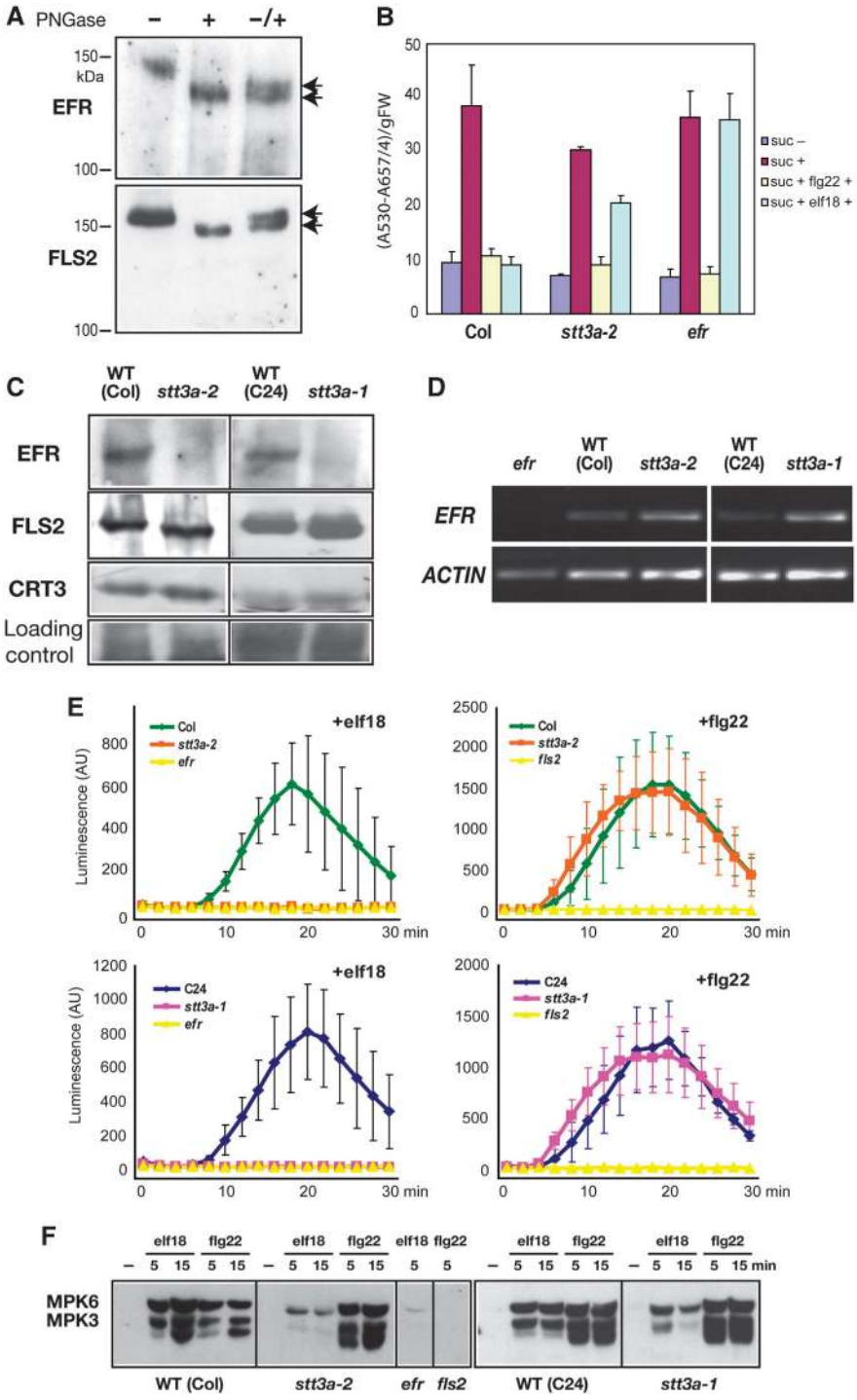

Figure 5 Accumulation and function of EFR, but not FLS2, are selectively impaired in the absence of STT3A-dependent N-glycosylation. (**A**) Peptide N-glycanase (PNGase) assay. Microsomal membrane fraction from non-elicited WT plants were digested with (+) or without (−) PNGase. An equal mixture of both samples was loaded onto the right lane (+/−). (**B**) Anthocyanin content in 6-day-old seedlings grown in the absence of sucrose (− Suc) or presence of 100 mM sucrose (+ Suc) without or with 1 μM flg22 (+ flg22) or elf18 (+ elf18). (**C**) Immunoblot analysis of microsomal membrane fraction from non-elicited leaves of 4-week-old plants with the indicated antibodies. (**D**) Semi-quantitative RT–PCR analysis for *EFR* expression in non-elicited leaves of 4-week-old plants. (**E**) ROS generation triggered in leaf discs derived from 4-week-old plant leaves on elf18 or flg22 at 100 nM. (**F**) MAPK activation in 2-week-old seedlings triggered by elf18 or flg22 at 1 μM for the indicated times.

range of phylogenetic lineages of higher plants including monocotyledonous and dicotyledonous plants that diverged approximately 200 million years ago. In contrast, elf18/elf26 responsiveness has been described only in the Brassicaceae to date (Boller and Felix, 2009). Thus, we propose that EFR is an evolutionarily young PRR that strictly requires stringent ERQC for its maturation. On the other hand, the evolutionary ancient FLS2 might have acquired redundant biogenesis pathways and/or autonomous folding capacity, thereby conferring robustness against disturbance in N-glycosylation.

It has been documented in mammals that gp96, an ER paralogue of HSP90, acts as a master chaperone for the

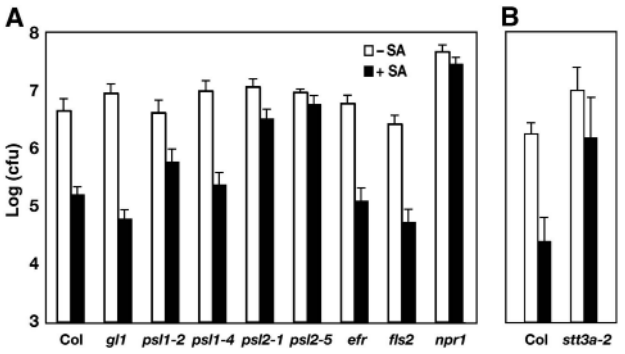

Figure 6 UGGT and STT3A are required for SA-induced, EFR/FLS2-independent defence. (**A**, **B**) Growth of *P. syringae* pv. *maculicola* (*Psm*) ES4326 in 25-day-old plants after the application of exogenous SA for defence induction. Plants were sprayed with (+SA) or without (−SA) 0.5 mM SA 24 h before infiltration with the bacteria at 5×10^5 cfu/ml. Leaf bacteria were quantified 3 days after inoculation.

membrane-resident PRRs toll-like receptors (TLRs) (Akashi-Takamura and Miyake, 2008). All five TLR members tested, acting either at the cell surface or in the EMs, show defects in their functions in the absence of gp96, suggesting a general function of this ER chaperone-mediated ERQC in the folding of TLRs (Yang *et al*, 2007). It will be interesting to investigate whether client-specific ERQC occurs in the biogenesis of individual TLRs that could contribute to their distinctive immune subfunctions.

Of note, the isolation of the *psl* mutants without pleiotropic defects highlights a difference in the function of the CRT/UGGT cycle between plants and mammals. In the latter, deletion of individual members results in embryonic lethality or premature death (Anelli and Sitia, 2008). As the upstream steps of the ER N-glycosylation pathway are also essential for plant development and growth (Boisson *et al*, 2001; Burn *et al*, 2002; Koiwa *et al*, 2003), a functional divergence might occur at the CRT/UGGT cycle (e.g. among different CRT/CNX members). The diversification of a subset of ERQC machineries, represented by the CRT3/UGGT cycle, might have facilitated the evolution of new RLK-type immune receptors, and thus represent a means by which plants deal with a wide range of pathogens in the absence of adaptive immunity.

Specific usage of quality control machineries for plant immune receptors is conceptually analogous to the earlier defined function of the cytosolic RAR1/SGT1/HSP90 chaperone complex for the abundance control of the intracellular NB-LRR class of R proteins (Shirasu, 2009). However, whether post-activated signalling of client R proteins is also under the control of this chaperone complex remains to be tested. It is important that in the weakly defective *psl1* (*crt3*) plants, EFR-signalling outputs are differentially rather than uniformly impaired despite WT-like EFR accumulation (Figure 4). This strongly points to a potential function of CRT3 in the modulation of client receptor-triggered signalling beyond the maintenance of recognition-competent receptor levels. Our data suggest that EFR receptor-ligand-binding activity is lower in *psl1-1* and *psl1-3* plants than in WT plants (Figure 4E and F). How can such lowered receptor-ligand binding lead to the observed differential impairment in EFR-signalling outputs (Figure 4B–D)? It is conceivable that greater amounts of a ligand-bound, signalling-active form of the receptor are required to induce callose deposits than ROS generation (threshold model). Alternatively, but not mutually exclusively, distinct receptor conformers are, respectively, responsible for branched signalling. In this scenario, a differential degree/rate of ligand binding on the LRR domain would serve to dictate such distinct states of the receptor. Impaired CRT3-assisted folding may thus fail to generate the full repertoire of receptor conformations such that PSL1-1 only supports the generation of an EFR state that is capable of intermediate-level ROS production, whereas PSL1-3 supports the generation of receptor states that activate nearly WT-like ROS production and MAPK activity, but still fail to fully induce callose deposition and repress anthocyanin accumulation, respectively (Figure 4B–D). Finally, it is also possible that ligand-binding activity and diverse EFR conformers are established through uncoupled processes that both require CRT3. Clearly, the weakly defective *crt3* alleles serve as future genetic tools to examine these earlier unsuspected mechanisms on how a single PRR governs multi-branched signalling pathways.

Materials and methods

Plant materials and growth conditions

Arabidopsis M2 population used for *psl* mutant screening is in the Col-0 *glabrous1* (*gl1*) mutant background (LEHLE seeds, TX USA). *efr-1*, *fls2*, *mpk3*, *mpk6* and *npr1-1* mutants have been described earlier (Zipfel *et al*, 2004, 2006; Wang *et al*, 2005; Takahashi *et al*, 2007). The WT control used was Col-0 unless otherwise stated. For the sucrose-MAMP crosstalk assays, seedlings were grown under constant light in liquid medium containing 0.5 × MS for 3 days and then for further 3 days with or without the addition of sucrose and MAMPs at the indicated concentrations. For MAPK/callose assays and *in vitro* MAMP cross-linking assays, seedlings were grown on 0.5 × MS agar plates or liquid medium, respectively, with 25 mM sucrose under 12 h light/12 h dark conditions for 10–14 days. Plants were grown on soil under 10 h light/14 h dark conditions for 4–5 weeks for ROS and bacterial spray infection assays, or under 12 h light/12 h dark conditions for 25 days for SA-induced resistance assays.

Immunoblot analysis

Microsomal membrane fractions were essentially prepared as described (Kinoshita *et al*, 1995), and then subjected to immunoblot analysis with the indicated antibodies to monitor PRRs and membrane proteins. The blots were stained with Coomassie blue to verify equal loading. The experiments were repeated at least three times essentially with the same conclusion. Representative results are shown. Quantification of immunoblots was performed with ImageJ (http://rsb.info.nih.gov/ij/). Band intensities were normalized with the value of background regions and then relative band intensities were calculated with that of each WT mock control (= 1.0).

MAMP assays

Anthocyanin content in whole seedlings was determined as described (Teng *et al*, 2005), using at least three sets of more than eight seedlings per treatment. ROS assays were conducted essentially as described earlier (Gomez-Gomez *et al*, 1999) with the following modifications. Leaf discs (5 mm diameter) excised from mature leaves were kept on water overnight before the luciferase-based measurement of ROS generation triggered by the addition of MAMPs. For MAPK and callose assays, the whole seedlings were applied with elf18 or flg22 at 1 μM for the indicated times. MAPK activation was detected by immunoblot analysis of soluble proteins extracted from the seedlings in a lysis buffer described earlier (Saijo *et al*, 2008), using anti-phospho p44/p42 MAPK antibody. Callose deposits were stained with aniline blue and visualized as described (Lipka *et al*, 2005).

Pathogen inoculation and growth assays

Bacterial inoculation assays were preformed as described earlier (Zipfel *et al*, 2004) with the following modifications. *Pst* DC3000 was sprayed onto leaf surface at 1×10^9 colony-forming unit (cfu)/ml. Infected plants were kept in a covered container for 3 days before harvesting leaves. A total of 12 surface-sterilized leaf discs

(5 mm diameter) excised from two leaves of six plants per genotype were randomly separated into three pools, and then subjected to the quantification of leaf bacteria. For SA-induced resistance assays, plants were sprayed with 0.5 mM SA or water 24 h before inoculation. *P. syringae* pv. *maculicola* (*Psm*) ES4326 suspension at 5×10^5 cfu/ml was syringe-infiltrated into 2–3 leaves of 12 plants per genotype per treatment. Three days post-inoculation, a leaf disc (6 mm diameter) was excised from 12 representative leaves per treatment. These 12 leaf discs were separated into 6 pools, and then used to determine bacterial titers. These experiments have been repeated three times with the same conclusion.

Antibodies

Anti-EFR sera were raised in rabbits (Eurogentec, Belgium) against the C-terminal 82 amino-acid (aa) residues (aa 950–1031) of EFR expressed as a $(His)_6$-tag fusion protein using a pET16b vector system (Novagen) in *E. coli*. Anti-CRT3 sera were raised in rabbits (Eurogentec) against the peptides ^{49}WKRNEGKAGTKFHT^{62} + C and C + ^{408}YKRPNPRDYMDDYHD^{422} of CRT3. Anti-CRT1 sera were raised in rabbits against the AtCRT1 peptide ^{394}GDDSDNESKSEET-KEAE^{410}. Anti-phospho p44/p42 MAPK antibody that specifically recognizes an active MAPK form was purchased from Cell Signaling Technology, MA, USA. Anti-FLS2 and AHA2 antibodies were described elsewhere (Kinoshita *et al*, 2001; Chinchilla *et al*, 2006).

Two-phase partitioning

Plant membrane protein fractionation was performed as described (Kinoshita *et al*, 1995) with the following modifications. Plant tissues were homogenized in a lysis buffer containing 50 mM Tris–HCl, pH 7.5, 5 mM EDTA, 0.3 M sucrose, 1.5% (w/v) insoluble polyvinylpyrrolidone, 5 mM DTT, 1 × Protease Inhibitor Cocktail (Roche), and 1 mM 4-(2-aminoethyl)benzenesulfonyl fluoride hydrochloride. Precipitates were collected by centrifuging the homogenates at 50 000 *g* for 40 min and suspending in a phosphate buffer containing 5 mM KH_2PO_4-KOH (pH 7.8), 5 mM KCl, 0.1 mM EDTA, 0.3 M sucrose, and 1 mM DTT (total microsomal membrane fraction). A measure of 4 g of two-phase solution containing 77.7 mg Dextran T500 and 77.7 mg PEG3350 in 844.7 mg of the phosphate buffer (per g) was used per 1 ml of the microsomal fraction. The upper phase was recovered from the two-phase partitioning mixture after the extraction cycle three times, diluted by five-fold with a Hepes buffer containing 5 mM Hepes-KOH pH 7.0, 0.3 M sucrose, and 1 mM DTT, and then centrifuged at 80 000 *g* for 40 min. The pellet was suspended in the Hepes buffer (PM-enriched fraction). The lower phase separated from the two-phase partitioning mixture was further subjected to the extraction cycle three times (EM-enriched fraction).

In vitro cross-linking assay

These were preformed essentially as described earlier (Chinchilla *et al*, 2006; Zipfel *et al*, 2006) with the following modifications. The above-ground portion of seedlings were ground and then suspended in respective binding buffers for elf26 and flg22. A 100 µl aliquots were incubated with 60 fmol elf26-^{125}I-Tyr or ^{125}I-Tyr-flg22 on ice for 15 or 25 min, respectively, either alone or in the presence of 10 µM unlabelled elf18 or flg22 peptides. Cross-linking was achieved by addition of 10 µl of 25 mM EGS (Pierce) and further incubation for 30 min at room temperature. After washing with fresh binding buffer, the resuspended samples were separated on SDS polyacrylamide gels, and then analysed using a Phosphoimager (Fuji FLA-7000). The results of gels analysed together are shown side by side. The gels were stained with Coomassie blue to verify equal loading. Experiments were repeated three times with similar results. For competitive binding assays, incubation on ice was followed by washing out unbound radio-labelled peptides by paper or glass fibre filters for elf26 and flg22 binding, respectively. Radioactivity retained on the filters was determined by scintillation counting, using scintillation fluid Rotiszint (Roth) and Beckmann Coulter LS 6500. Box plots were obtained using Systat software.

Table I Oligonucleotide sequences and restriction enzymes (RE) used as cleaved amplified polymorphic sequence markers to determine mutant genotypes

Allele	RE	Oligonucleotide sequences (5′-3′)	
psl1-1	*Hae* III	gacttgcgaactccatgtctt	tgaatccgaatccatccttc
psl1-2	*Scr* FI	ttttcttcctcgtcccagtc	acgatgtcaaacccgaggta
psl1-3	*Scr* FI	ttttcttcctcgtcccagtc	acgatgtcaaacccgaggta
psl1-4	*Mse* I	atataatagcatgcagaaaatcca	agggttgaaaacaaaaccaaaa
psl2-1	*Bfu* CI	gctttgaacagggtttctgg	tgtgaccaccaaagaaaggtt
psl2-2	*Alu* I	tgaatgctcgcaaaatgaaa	agaggatcagaggcatggac

Treatment of Arabidopsis seedlings with ERAD inhibitors

Two-week-old hydroponically grown seedlings were incubated in the liquid medium (0.5 × MS, 25 mM sucrose) containing 40 µM Kifunensine (Sigma) and 20 µM MG132 (Sigma) for 24 h, and then subjected to immunoblot analysis or MAPK assays.

PNGase treatment

Microsomal membrane fraction prepared from non-elicited 4-week-old plants was suspended in 0.1% NP40, and then subjected to digestion with PNGase F (New England Biolabs) according to the manufacturer's instructions.

RT–PCR analysis

Total RNA was isolated from a portion of plant tissues used for immunoblot analysis, and then subjected to semi-quantitative RT–PCR analysis for *EFR* (At5g20480) and *ACTIN1* (At2g37620) expression. We verified the exponential amplification of both products without saturation in PCRs at 24, 28, and 32 cycles. The results at 28 cycles are shown. Gene-specific primers used are as follows.

EFR: 5′-AATATTTGCGGAGGCGTCCG-3′ 5′-AATGAACGTGCAGAT ACTCC-3′

ACTIN1: 5′-TGCGACAATGGAACTGGAATG-3′ 5′-CTGTCTCGAGT TCCTGCTCG-3′

Cloning of PSL1 and PSL2 genes

PSL1 and *PSL2* genes were mapped with standard PCR-based marker procedures using F2 populations derived from Col *psl1-4* x Landsberg *erecta* (Ler), or Col *psl2-1* x Ler and Col *psl2-2* x Ler, respectively. Oligonucleotide sequences and restriction enzymes (RE) used to detect cleaved amplified polymorphic sequence markers for all mutant genotypes are shown in Table I.

Supplementary data

Supplementary data are available at *The EMBO Journal* Online (http://www.embojournal.org).

Acknowledgements

We thank T Kinoshita for suggestions on membrane protein preparation and anti-AHA2 antibodies, S Persson for anti-CRT1 antibodies, C Zipfel for *efr-1* seeds, K Shinozaki for *mpk3* and *mpk6* seeds, M Koornneef for C24 seeds, and M Vetter and M Kalda for technical assistance. The work was supported in part by the Max Planck Society, grants from SFB670 (PS-L and SR) and PhD fellowships from the IMPRS program (NT and XL).

Conflict of interest

The authors declare that they have no conflict of interest.

References

Akashi-Takamura S, Miyake K (2008) TLR accessory molecules. *Curr Opin Immunol* **20:** 420–425

Anelli T, Sitia R (2008) Protein quality control in the early secretory pathway. *EMBO J* **27:** 315–327

Asai T, Tena G, Plotnikova J, Willmann MR, Chiu WL, Gomez-Gomez L, Boller T, Ausubel FM, Sheen J (2002) MAP kinase signalling cascade in Arabidopsis innate immunity. *Nature* **415:** 977–983

Asselbergh B, De Vleesschauwer D, Hofte M (2008) Global switches and fine-tuning-ABA modulates plant pathogen defense. *Mol Plant Microbe Interact* **21:** 709–719

Boisson M, Gomord V, Audran C, Berger N, Dubreucq B, Granier F, Lerouge P, Faye L, Caboche M, Lepiniec L (2001) Arabidopsis glucosidase I mutants reveal a critical role of N-glycan trimming in seed development. *EMBO J* **20:** 1010–1019

Boller T, Felix G (2009) A renaissance of elicitors: perception of microbe-associated molecular patterns and danger signals by pattern-recognition receptors. *Annu Rev Plant Biol* **60:** 379–406

Burn JE, Hurley UA, Birch RJ, Arioli T, Cork A, Williamson RE (2002) The cellulose-deficient Arabidopsis mutant rsw3 is defective in a gene encoding a putative glucosidase II, an enzyme processing N-glycans during ER quality control. *Plant J* **32:** 949–960

Chinchilla D, Bauer Z, Regenass M, Boller T, Felix G (2006) The Arabidopsis receptor kinase FLS2 binds flg22 and determines the specificity of flagellin perception. *Plant Cell* **18:** 465–476

Chinchilla D, Zipfel C, Robatzek S, Kemmerling B, Nurnberger T, Jones JD, Felix G, Boller T (2007) A flagellin-induced complex of the receptor FLS2 and BAK1 initiates plant defence. *Nature* **448:** 497–500

Chisholm ST, Coaker G, Day B, Staskawicz BJ (2006) Host-microbe interactions: shaping the evolution of the plant immune response. *Cell* **124:** 803–814

Clay NK, Adio AM, Denoux C, Jander G, Ausubel FM (2009) Glucosinolate metabolites required for an Arabidopsis innate immune response. *Science* **323:** 95–101

Felix G, Duran JD, Volko S, Boller T (1999) Plants have a sensitive perception system for the most conserved domain of bacterial flagellin. *Plant J* **18:** 265–276

Gomez-Gomez L, Felix G, Boller T (1999) A single locus determines sensitivity to bacterial flagellin in Arabidopsis thaliana. *Plant J* **18:** 277–284

Hebert DN, Molinari M (2007) In and out of the ER: protein folding, quality control, degradation, and related human diseases. *Physiol Rev* **87:** 1377–1408

Heese A, Hann DR, Gimenez-Ibanez S, Jones AM, He K, Li J, Schroeder JI, Peck SC, Rathjen JP (2007) The receptor-like kinase SERK3/BAK1 is a central regulator of innate immunity in plants. *Proc Natl Acad Sci USA* **104:** 12217–12222

Hong Z, Jin H, Tzfira T, Li J (2008) Multiple mechanism-mediated retention of a defective brassinosteroid receptor in the endoplasmic reticulum of Arabidopsis. *Plant Cell* **20:** 3418–3429

Jin H, Yan Z, Nam KH, Li J (2007) Allele-specific suppression of a defective brassinosteroid receptor reveals a physiological role of UGGT in ER quality control. *Mol Cell* **26:** 821–830

Jones JD, Dangl JL (2006) The plant immune system. *Nature* **444:** 323–329

Kim MG, da Cunha L, McFall AJ, Belkhadir Y, DebRoy S, Dangl JL, Mackey D (2005) Two pseudomonas syringae type III effectors inhibit RIN4-regulated basal defense in Arabidopsis. *Cell* **121:** 749–759

Kinoshita T, Doi M, Suetsugu N, Kagawa T, Wada M, Shimazaki K (2001) Phot1 and phot2 mediate blue light regulation of stomatal opening. *Nature* **414:** 656–660

Kinoshita T, Nishimura M, Shimazaki K (1995) Cytosolic concentration of Ca2+ regulates the plasma membrane H+-ATPase in guard cells of Fava bean. *Plant Cell* **7:** 1333–1342

Koiwa H, Li F, McCully MG, Mendoza I, Koizumi N, Manabe Y, Nakagawa Y, Zhu J, Rus A, Pardo JM, Bressan RA, Hasegawa PM (2003) The STT3a subunit isoform of the Arabidopsis oligosaccharyltransferase controls adaptive responses to salt/osmotic stress. *Plant Cell* **15:** 2273–2284

Kunze G, Zipfel C, Robatzek S, Niehaus K, Boller T, Felix G (2004) The N terminus of bacterial elongation factor Tu elicits innate immunity in Arabidopsis plants. *Plant Cell* **16:** 3496–3507

Lipka V, Dittgen J, Bednarek P, Bhat R, Wiermer M, Stein M, Landtag J, Brandt W, Rosahl S, Scheel D, Llorente F, Molina A, Parker J, Somerville S, Schulze-Lefert P (2005) Pre- and postinvasion defenses both contribute to nonhost resistance in Arabidopsis. *Science* **310:** 1180–1183

Lo SC, Nicholson RL (1998) Reduction of light-induced anthocyanin accumulation in inoculated sorghum mesocotyls. Implications for a compensatory role in the defense response. *Plant Physiol* **116:** 979–989

Loake G, Grant M (2007) Salicylic acid in plant defence—the players and protagonists. *Curr Opin Plant Biol* **10:** 466–472

Lozoya E, Block A, Lois R, Hahlbrock K, Scheel D (1991) Transcriptional repression of light-induced flavonoid synthesis by elicitor treatment of cultured parsley cells. *Plant J* **1:** 227–234

McLusky SR, Bennett MH, Beale MH, Lewis MJ, Gaskin P, Mansfield JW (1999) Cell wall alterations and localized accumulation of feruloyl-3′-methoxytyramine in onion epidermis at sites of attempted penetration by Botrytis allii are associated with actin polarisation, peroxydase activity and suppression of flavonoid biosynthesis. *Plant J* **17:** 523–534

Mishina TE, Zeier J (2007) Pathogen-associated molecular pattern recognition rather than development of tissue necrosis contributes to bacterial induction of systemic acquired resistance in Arabidopsis. *Plant J* **50:** 500–513

Nekrasov V, Li J, Batoux M, Roux M, Chu Z-H, Lacombe S, Rougon A, Bittel P, Kiss-Papp M, Chinchilla D, van Esse HP, Jorda L, Schwessinger B, Nicaise V, Thomma BPHJ, Molina A, Jones JDG, Zipfel C (2009) Control of the pattern-recognition receptor EFR by an ER protein complex in plant immunity. *EMBO J* (e-pub ahead of print 17 September 2009; doi:10.1038/emboj.2009.262)

Pattison RJ, Amtmann A (2009) N-glycan production in the endoplasmic reticulum of plants. *Trends Plant Sci* **14:** 92–99

Persson S, Rosenquist M, Svensson K, Galvao R, Boss WF, Sommarin M (2003) Phylogenetic analyses and expression studies reveal two distinct groups of calreticulin isoforms in higher plants. *Plant Physiol* **133:** 1385–1396

Saijo Y, Zhu D, Li J, Rubio V, Zhou Z, Shen Y, Hoecker U, Wang H, Deng XW (2008) Arabidopsis COP1/SPA1 complex and FHY1/FHY3 associate with distinct phosphorylated forms of phytochrome A in balancing light signaling. *Mol Cell* **31:** 607–613

Shen QH, Saijo Y, Mauch S, Biskup C, Bieri S, Keller B, Seki H, Ulker B, Somssich IE, Schulze-Lefert P (2007) Nuclear activity of MLA immune receptors links isolate-specific and basal disease-resistance responses. *Science* **315:** 1098–1103

Shirasu K (2009) The HSP90-SGT1 chaperone complex for NLR immune sensors. *Annu Rev Plant Biol* **60:** 139–164

Takahashi F, Yoshida R, Ichimura K, Mizoguchi T, Seo S, Yonezawa M, Maruyama K, Yamaguchi-Shinozaki K, Shinozaki K (2007) The mitogen-activated protein kinase cascade MKK3-MPK6 is an important part of the jasmonate signal transduction pathway in Arabidopsis. *Plant Cell* **19:** 805–818

Teng S, Keurentjes J, Bentsink L, Koornneef M, Smeekens S (2005) Sucrose-specific induction of anthocyanin biosynthesis in Arabidopsis requires the MYB75/PAP1 gene. *Plant Physiol* **139:** 1840–1852

Tsuda K, Sato M, Glazebrook J, Cohen JD, Katagiri F (2008) Interplay between MAMP-triggered and SA-mediated defense responses. *Plant J* **53:** 763–775

Tsukaya H, Ohshima T, Naito S, Chino M, Komeda Y (1991) Sugar-dependent expression of the CHS-A gene for chalcone synthase from petunia in transgenic Arabidopsis. *Plant Physiol* **97:** 1414–1421

Wang D, Weaver ND, Kesarwani M, Dong X (2005) Induction of protein secretory pathway is required for systemic acquired resistance. *Science* **308:** 1036–1040

Yang Y, Liu B, Dai J, Srivastava PK, Zammit DJ, Lefrancois L, Li Z (2007) Heat shock protein gp96 is a master chaperone for toll-like receptors and is important in the innate function of macrophages. *Immunity* **26:** 215–226

Yasuda M, Ishikawa A, Jikumaru Y, Seki M, Umezawa T, Asami T, Maruyama-Nakashita A, Kudo T, Shinozaki K, Yoshida S, Nakashita H (2008) Antagonistic interaction between systemic acquired resistance and the abscisic acid-mediated abiotic stress response in Arabidopsis. *Plant Cell* **20:** 1678–1692

Zhang J, Shao F, Li Y, Cui H, Chen L, Li H, Zou Y, Long C, Lan L, Chai J, Chen S, Tang X, Zhou JM (2007) A Pseudomonas syringae effector inactivates MAPKs to suppress PAMP-induced immunity in plants. *Cell Host Microbe* **1:** 175–185

Zipfel C, Kunze G, Chinchilla D, Caniard A, Jones JD, Boller T, Felix G (2006) Perception of the bacterial PAMP EF-Tu by the receptor EFR restricts Agrobacterium-mediated transformation. *Cell* **125:** 749–760

Zipfel C, Robatzek S, Navarro L, Oakeley EJ, Jones JD, Felix G, Boller T (2004) Bacterial disease resistance in Arabidopsis through flagellin perception. *Nature* **428:** 764–767